Global Biogeochemical Cycles

RESEARCH ARTICLE
10.1029/2023GB007994

Relationships Between Plankton Size Spectra, Net Primary Production, and the Biological Carbon Pump

Michael R. Stukel[1,2], Moira Décima[3], Thomas B. Kelly[1], Michael R. Landry[3], Scott D. Nodder[4], Mark D. Ohman[3], Karen E. Selph[5], and Natalia Yingling[1]

[1]Department of Earth, Ocean, and Atmospheric Science, Florida State University, Tallahassee, FL, USA, [2]Center for Ocean-Atmospheric Prediction Studies, Florida State University, Tallahassee, FL, USA, [3]Scripps Institution of Oceanography, University of California San Diego, La Jolla, SA, USA, [4]National Institute of Water and Atmospheric Research (NIWA), Wellington, New Zealand, [5]Department of Oceanography, University of Hawaii at Manoa, Honolulu, HI, USA

Abstract Photosynthesis in the surface ocean and subsequent export of a fraction of this fixed carbon leads to carbon dioxide sequestration in the deep ocean. Ecological relationships among plankton functional groups and theoretical relationships between particle size and sinking rate suggest that carbon export from the euphotic zone is more efficient when communities are dominated by large organisms. However, this hypothesis has never been tested against measured size spectra spanning the >5 orders of magnitude found in plankton communities. Using data from five ocean regions (California Current Ecosystem, North Pacific subtropical gyre, Costa Rica Dome, Gulf of Mexico, and Southern Ocean subtropical front), we quantified carbon-based plankton size spectra from heterotrophic bacteria to metazoan zooplankton (size class cutoffs varied slightly between regions) and their relationship to net primary production and sinking particle flux. Slopes of the normalized biomass size spectra (NBSS) varied from −1.6 to −1.2 (median slope of −1.4 equates to large 1–10 mm organisms having a biomass equal to only 7.6% of the biomass in small 1–10 μm organisms). Net primary production was positively correlated with the NBSS slope, with a particularly strong relationship in the microbial portion of the size spectra. While organic carbon export co-varied with NBSS slope, we found only weak evidence that export efficiency is related to plankton community size spectra. Multi-variate statistical analysis suggested that properties of the NBSS added no explanatory power over chlorophyll, primary production, and temperature. Rather, the results suggest that both plankton size spectra and carbon export increase with increasing system productivity.

Plain Language Summary Plankton communities in the open ocean are incredibly diverse taxonomically and with respect to size. They include bacteria smaller than 0.5 μm and metazoan zooplankton greater than 10-cm long. Organism size puts strong physiological constraints on many species; hence, changes in the relative sizes of plankton communities are predicted to correlate with important ecosystem functions, including photosynthesis rates, efficiency of food-web energy transfer, and carbon sequestration in the deep ocean by sinking organic particles. However, few studies have quantified the full size spectra of plankton communities across different marine ecosystems and none have concurrently measured photosynthesis and carbon export rates. We compiled plankton size spectra from the tropics to the Southern Ocean using consistent methods for bacteria, protists, and multicellular zooplankton. Size spectra slopes, which compare the relative biomass of large and small organisms, are slightly less than negative one, indicating that larger size classes contain less biomass than smaller ones. Ecosystems with higher photosynthetic rates are dominated by larger organisms and support a stronger biological carbon pump, transporting more carbon to the deep ocean. However, at similar levels of productivity, ecosystems with larger organisms do not transport significantly more carbon to the deep ocean than those dominated by smaller plankton.

Key Points:

- Normalized biomass size spectra (NBSS) slopes spanning bacteria to zooplankton ranged from −1.6 to −1.2 across diverse ocean regions
- Whole community NBSS slope, microbial NBSS slope, and zooplankton:microbe ratio were positively correlated with net primary production
- NBSS slope was positively correlated with sinking carbon export but was not significantly correlated with export efficiency

Supporting Information:

Supporting Information may be found in the online version of this article.

Correspondence to:

M. R. Stukel,
mstukel@fsu.edu

Citation:

Stukel, M. R., Décima, M., Kelly, T. B., Landry, M. R., Nodder, S. D., Ohman, M. D., et al. (2024). Relationships between plankton size spectra, net primary production, and the biological carbon pump. *Global Biogeochemical Cycles*, *38*, e2023GB007994. https://doi.org/10.1029/2023GB007994

Received 6 OCT 2023
Accepted 19 MAR 2024

Author Contributions:

Conceptualization: Michael R. Stukel
Formal analysis: Michael R. Stukel
Funding acquisition: Michael R. Stukel, Moira Décima, Michael R. Landry, Scott D. Nodder, Mark D. Ohman, Karen E. Selph
Investigation: Michael R. Stukel, Moira Décima, Thomas B. Kelly, Michael R. Landry, Scott D. Nodder, Mark D. Ohman, Karen E. Selph, Natalia Yingling
Writing – original draft: Michael R. Stukel
Writing – review & editing: Moira Décima, Thomas B. Kelly, Michael R. Landry, Scott D. Nodder, Mark D. Ohman, Karen E. Selph, Natalia Yingling

1. Introduction

The biological carbon pump (BCP) transports organic carbon (OC) fixed by phytoplankton in the sunlit surface ocean into the deep ocean, where it is converted to dissolved carbon constituents that can be sequestered for decades to millennia (Boyd et al., 2019; Ducklow et al., 2001; Volk & Hoffert, 1985). The BCP is an emergent process driven by ecological interactions among diverse taxa from all domains of life and ranging in size from approximately 10 fg C individual^{-1} (heterotrophic bacteria) to >1 kg C individual^{-1} (nekton). The complexity of

these interactions and their variability in space and time obfuscate simple relationships between phytoplankton production and carbon export and complicate our ability to predict future BCP changes (Burd et al., 2016; Siegel et al., 2016). Many studies suggest that the BCP is driven primarily by sinking particles (Buesseler & Boyd, 2009; Martin et al., 1987; Nowicki et al., 2022), although active transport mediated by vertically migrating organisms (Archibald et al., 2019; Longhurst et al., 1990; Steinberg et al., 2000) and passive flux driven by vertical mixing and water mass subduction can also be important (Carlson et al., 1994; Levy et al., 2013; Omand et al., 2015; Stukel & Ducklow, 2017).

The efficiency of the BCP is impacted by the composition, structure and size spectra of planktonic organisms (Boyd & Newton, 1999; Henson et al., 2022; Jackson et al., 2005; Serra-Pompei et al., 2022; Stemmann & Boss, 2011). Large phytoplankton sink more rapidly as individuals than picophytoplankton (Smayda, 1971). They are also more likely to aggregate into marine snow (Alldredge & Gotschalk, 1989; Scharek et al., 1999; Thornton, 2002) and to be consumed by fecal pellet-producing metazoan zooplankton (Michaels & Silver, 1988; Steinberg & Landry, 2017). Similarly, the size and sinking rates of zooplankton fecal pellets are correlated with the size of the organisms that egest them (Small et al., 1979; Stamieszkin et al., 2015; Turner, 2015). Conversely, submicron-sized heterotrophic bacteria and archaea are believed to primarily play roles as remineralizers, thus decreasing flux into the deep ocean (Kellogg et al., 2011; Mislan et al., 2014; Steinberg et al., 2008), although there is evidence that small-sized organisms can also be incorporated into sinking marine snow aggregates and fecal pellets and contribute to carbon export (Richardson, 2019; Waite et al., 2000). Indeed, a recent global three-dimensional size-structured model suggests that the slopes of plankton size spectra may be the best predictor of carbon flux efficiency into the deep ocean (Serra-Pompei et al., 2022). This hypothesis has yet to be tested with in situ data, however, due to the paucity of studies that have simultaneously quantified plankton biomass across multiple orders of magnitude in body size while also measuring carbon export from the surface ocean.

In this study, we compile size spectra measurements spanning picoplankton (0.5–2.0 μm) to >5-mm macrozooplankton from multiple regions in the world ocean (California coastal upwelling biome, North Pacific subtropical gyre, Costa Rica Dome (CRD), Gulf of Mexico (GoM), and Southern Ocean subtropical front). These measurements, made using a suite of consistent methods in regions from the tropics to the Southern Ocean, are paired with floating sediment trap and ^{234}Th measurements of particle flux out of the euphotic zone. We utilize the slope of the normalized biomass size spectrum (NBSS) as a measure of the relative contributions of large and small plankton to community biomass. The NBSS linear slope is a widely used metric for quantifying spatio-temporal patterns in the plankton community size structure (Fry & Quiñones, 1994; Quiñones et al., 2003; Rodriguez & Mullin, 1986; Rykaczewski, 2019), with steeper (more negative) slopes indicating relative dominance by small plankton and shallower (less negative) slopes indicating relative dominance by large plankton. While many regional studies have measured NBSS slopes for either phytoplankton size classes (typically <200 μm) or zooplankton size classes (typically >200 μm), far fewer have quantified the NBSS across the full size range in plankton communities. Here we utilize flow cytometry, epifluorescence microscopy, and zooplankton net tow results made consistently across five oceanic regions to test two hypotheses: (a) The slope of the NBSS is less steep (i.e., dominance by larger plankton) when ecosystem productivity (defined as net primary production [NPP]) is high; and (b) the efficiency of the BCP (defined as the ratio of sinking particle flux to NPP) is higher when the community is dominated by large plankton (i.e., export efficiency correlates positively with NBSS slope). We further investigate the relationships between the phytoplankton and zooplankton size spectra and ask whether plankton size spectra are statistically useful predictors of carbon export rates.

2. Materials and Methods

2.1. Measurements

In situ data were compiled from five field programs (Figure 1). Datasets from the California Current Ecosystem Long-Term Ecological Research (CCE LTER) Program are derived from eight cruises spanning multiple seasons and years in the southern sector of the California Current System. This region includes a productivity gradient stretching from a coastal upwelling biome to an oligotrophic offshore domain (Ohman et al., 2013). Results from the CRD were derived from the CRD FLUxes and ZInc Experiments (FLUZIE) cruise in an open-ocean upwelling region of the Eastern Tropical Pacific in July 2010 (Landry et al., 2016). The GoM dataset was collected on two cruises of the Bluefin Larvae in Oligotrophic Ocean Foodwebs, Investigations of Nutrients to Zooplankton (BLOOFINZ-GoM) program in May 2017 and May 2018 that focused on the oligotrophic deepwater spawning

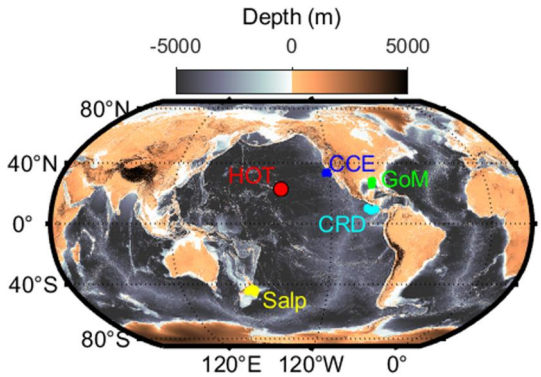

Figure 1. Locations of Lagrangian experiments in the California Current Ecosystem (CCE), Gulf of Mexico (GoM), Costa Rica Dome (CRD), and Southern Ocean subtropical front (Salp), as well as station ALOHA, the sampling site for the Hawaii Ocean Time-series (HOT).

grounds of Atlantic Bluefin Tuna (Gerard et al., 2022). The Salp Particle expOrt and Oceanic Production (SalpPOOP) Expedition investigated the Southern Ocean region near the Subtropical Front and sampled waters of frontal, subtropical and subantarctic origin (Décima et al., 2023). All of these programs utilized quasi-Lagrangian sampling schemes with Lagrangian experiments that lasted from ∼2.25 to ∼7.75 days in duration (typical duration = 4.25 days) allowing repeated sampling of plankton communities from bacteria to microzooplankton within distinct water parcels (Landry, 2009). Samples from the North Pacific Subtropical Gyre were collected by the Hawaii Ocean Time-series (HOT) program, which samples the time-series station ALOHA over ∼3 days near Hawai'i with ∼monthly frequency (Church et al., 2013; Karl & Church, 2014). Brief descriptions of field methods are given below. Additional details are available in original publications as cited.

2.1.1. Microbes

Samples for microbial biomass were collected using Niskin bottles at 6–8 depths spanning the euphotic zone. Picoplankton abundances (heterotrophic bacteria, *Prochlorococcus*, *Synechococcus*, and picoeukaryotes) were determined by flow cytometry and converted to biomass using carbon cell^{-1} conversion factors for their respective regions as determined by the original investigators (Selph et al., 2016, 2021). While conversion factors did vary slightly between regions for some groups, they were generally quite similar. Nano- and microplankton biomasses were determined by epifluorescence microscopy with proflavin (protein) and DAPI (nucleic acid) staining (Taylor et al., 2012, 2016). 50-mL samples were filtered through 0.8-µm filters to quantify ∼2- to 12-µm cells (imaged at 60× or 63× magnification) and 450-mL samples were filtered through 8.0-µm filters to quantify >12-µm cells (imaged at 20× magnification). Cells were manually outlined based on proflavin fluorescence and carbon biomass was determined from biovolume using equations in Menden-Deuer and Lessard (2000). We note that while this approach will accurately quantify most nano- and micro-sized protists (autotrophic, heterotrophic, and mixotrophic), some fragile taxa (e.g., some ciliates) may not survive preservation and hence could be undercounted.

2.1.2. Mesozooplankton

Mesozooplankton were collected with either a ring net or a bongo net with 202-µm mesh, equipped with a General Oceanics flow meter and a depth sensor. Double oblique net tows (to a maximum depth between 100 and 210 m) were conducted twice daily (paired day and night tows) during Lagrangian experiments. Typically, 3-day-night pairs of tows were conducted for each occupation of Station ALOHA in the subtropical North Pacific. After recovery, samples were split using a Folsom splitter and sequentially filtered through nested sieves (5, 2, 1, 0.5, 0.2 mm). Sieves were rinsed onto pre-weighed, 47-mm diameter, 0.2-mm mesh filters, rinsed with isotonic ammonium formate, and dried for storage (Décima et al., 2016; Landry & Swalethorp, 2021). On land, samples were weighed to determine dry mass. Filters from most projects were then subsampled for C/N analyses by an elemental analyzer, thus providing carbon values for all five size classes. For cruises without direct carbon measurements available, dry weight was converted to carbon using the equations in Landry et al. (2001). On the SalpPOOP cruise, >5-mm salps were removed from the >5-mm sample and individually sized (for all other cruises, no organisms were removed from the large size fraction and it was treated identically to other size fractions). We estimated salp biomass using allometric relationships in Iguchi and Ikeda (2004) and included it in the >5-mm sample.

2.1.3. Net Primary Production

NPP was measured by incorporation of ^{13}C or ^{14}C labeled bicarbonate (Morrow et al., 2018; Yingling et al., 2022). During Lagrangian experiments, NPP was measured at 6–8 depths spanning the euphotic zone in polycarbonate bottles incubated in situ at the collection depth for ∼24 hr on an in situ array to ensure natural light and temperature (Landry et al., 2009). After recovery, samples were collected, filtered and analyzed by either liquid scintillation counting (for ^{14}C) or isotope ratio mass spectrometry (for ^{13}C). Experiments were conducted daily and vertically integrated over the euphotic zone. At Station ALOHA in the subtropical North Pacific, NPP

measurements were made in deckboard incubators simulating conditions at 8 depths spanning the euphotic zone (Karl & Church, 2014).

2.1.4. Carbon Export

Sinking particulate OC flux was measured using short-term (2- to 5-day) deployments of surface-tethered VERTEX-style sediment traps (Karl et al., 1996; Knauer et al., 1979; Stukel et al., 2021), typically at multiple depths from the base of the euphotic zone through the twilight zone to depths of 300–500 m. Sediment trap tubes (70-mm inner diameter, 8:1 aspect ratio, baffled) were deployed with a preserved saltwater brine (filtered seawater amended with 50 g L^{-1} NaCl and 0.4% formaldehyde, final concentration). After recovery, the overlying water was removed by gentle suction and samples were manually inspected to remove the metazoan "swimmers." Samples were then split on a Folsom splitter (if necessary) and filtered through pre-combusted glass fiber filters. Filters were acidified prior to analysis on an elemental analyzer to determine OC and nitrogen (N) contents. For one cruise in the California Current (CCE-P0605), sediment traps were not available and export was measured by ^{234}Th-^{238}U-disequilibrium (Stukel et al., 2011). Extensive simultaneous use of sediment traps and ^{234}Th-^{238}U-disequilibrium in the California Current Ecosystem (CCE) have shown good agreement between these methods for our specific deployment methods (Stukel et al., 2019). For the CCE, CRD, GoM, and SalpPOOP datasets, carbon export was extrapolated to the depth of the euphotic zone (defined as the 0.1% incident light level) using a power law fit (Martin et al., 1987). Results were relatively insensitive to this extrapolation, because the shallowest sediment trap depth was typically near the depth of the euphotic zone. On the CCE-P0704 and CCE-P0605 cruises, export flux was only measured at 100 m depth and a power law exponent of $b = 0.72$ was used (calculated average for the CCE region, Stukel et al., 2023). For the Station ALOHA data, we assumed that the 150-m sediment trap results were representative of carbon export at the 0.1% light level, because photosynthetically active radiation data were not publicly available. This seems like a reasonable estimate because 90% of primary production occurs in the upper 100 m at this site (Karl et al., 1996).

2.2. Data Treatment

We compiled flow cytometry, epifluorescence microscopy, and zooplankton net tow data to compute normalized biomass size spectra (NBSS, Figure 2). The NBSS is defined by taking the biomass within a size bin (units = mmol C m^{-3}) and dividing by the width of that size bin (units = μm). It is thus theoretically independent of the choice of size bins. Our choice of size bins was dictated by the size bins reported by each field program, which typically followed approximately octave (base 2) scaling. However, we were forced to make some distinct choices: (a) Cell size was not reported for flow cytometry data, hence we assumed that the size bin for picoplankton was 0.5–2.0 μm. This is likely a reasonable range that encompasses most biomass for populations including heterotrophic bacteria, *Prochlorococcus*, *Synechococcus*, and picoeukaryotes. (b) The largest size class of microplankton reported from epifluorescence microscopy data was typically either >20 μm or >40 μm. We assumed that this size class extends to an upper limit of 200-μm cells, because many common protists (e.g., diatoms, dinoflagellates, and ciliates) seen in these samples can reach this size. However, we acknowledge that epifluorescence microscopy likely misses many <200-μm metazoan zooplankton (e.g., appendicularians and copepod nauplii that are likely common in all study regions) as well as fragile rhizarians (that are known to be common and contribute to export in the CCE region, Gutierrez-Rodriguez et al., 2019). Our estimate of the biomass of this size class is thus likely an underestimate. (c) The upper limit of the >5-mm mesozooplankton size class is also unknown. We consistently treated this size class as encompassing organisms from 5 to 50 mm because 50 mm was a reasonable estimate for the upper limit of organisms typically collected in this size class. However, functionally this class includes all >5 mm taxa that were present and did not avoid the net. For instance, the "5–50 mm" size class often included ∼100 mm salps in the SalpPOOP study and 50–200 mm pyrosome colonies in the CCE. While it might have been most appropriate to remove all >50 mm organisms from this size class, this was not possible as the proportion of the biomass contained in >50 mm organisms was not included in the datasets. Furthermore, since our goal was to estimate the slope of the plankton size spectrum, the exclusion of all large mesozooplankton would bias our results. We thus consider it most appropriate to sum all >5-mm taxa into a single size class and use a typical maximum size (50 mm) as the assumed upper limit of the bin.

To compute the NBSS, we first determined the average euphotic zone biomass in each bin size. For microbial populations, we vertically integrated the biomass profiles from 6 to 8 depths through the euphotic zone. We then divided by the depth of the deepest sample (which was always near the base of the euphotic zone) to determine an

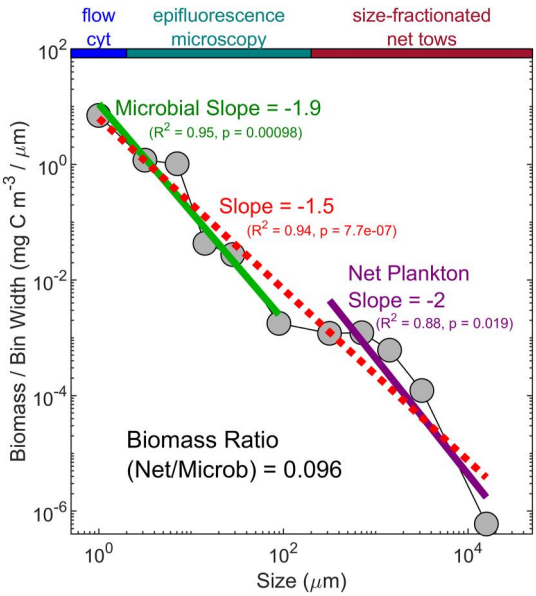

Figure 2. Example of the Normalized Biomass Size Spectrum (NBSS) with data from the first Lagrangian experiment in the 2017 BLOOFINZ-GoM cruise. Dashed line is the Ordinary Least Squares (OLS) regression for the entire NBSS. Solid lines represent OLS regressions for the microbial (<200 μm) and net-collected (>200 μm) portions of the plankton community. Both OLS regressions were computed on log-transformed data. The biomass ratio is the ratio of the summed net plankton carbon biomass (Net) divided by the summed microbial carbon biomass (Microb).

average volumetric carbon biomass (mmol C m^{-3}). Multiple profiles per Lagrangian experiment were averaged. For mesozooplankton size classes, volumetric carbon biomass was determined by dividing the net-tow biomass by the volume filtered (determined using a flow meter attached to the net frame). For each Lagrangian experiment, we computed daytime and nighttime average biomasses and then took the average of these two values to get a day-night mean estimate of volumetric carbon biomass. Individual microbial size classes thus typically incorporated ∼24 distinct measurements (6 depths × 4 days for one Lagrangian experiment), while zooplankton size classes typically incorporated eight distinct measurements (∼2 paired day and night tows per day × 4 days). We believe this results in very robust estimates of the NBSS for these programs. For the station ALOHA samples, results are typically derived from a single profile of microbial measurements (Pasulka et al., 2013) and three day-night pairs of zooplankton net tows and hence should be assumed to have greater uncertainty.

2.3. Statistical Analyses

To quantify NBSS slopes as an index of relative contributions of large and small organisms to community biomass, we used ordinary least squares regression (OLS). OLS was chosen with the justification that size classes (independent variables) were controlled in the original analyses such that organism size uncertainties were very small compared to uncertainties in size class biomass in the field samples. The use of OLS also allowed consistency with other NBSS studies. For all other linear regressions (e.g., regressions of NBSS against environmental parameters) we used Type II (geometric mean) linear regressions, because neither variable was controlled nor measured without uncertainty. To investigate parameter interdependencies, we used Spearman's rank correlation, which does not assume linearity between the tested parameters, but rather tests whether their relationship can be described by a monotonic function. Geometric mean regressions were only plotted on figures if the Spearman's rank correlation was significant at the 95% confidence level.

We used Least Absolute Shrinkage and Selection Operator (LASSO) regressions for variable selection and linear model development using the function "lasso" in Matlab R2022b. LASSO was chosen because our data exhibited substantial multicollinearity. LASSO was implemented using 10-fold cross validation. To choose an appropriate λ value, we used the common criterion of choosing the lambda that led to the sparsest model within one standard error of the minimum mean squared error. Variables that followed an approximately log-normal distribution were log transformed prior to analyses. These included carbon export, NPP, surface chlorophyll, and the ratio of net plankton to microbial biomass.

3. Results

3.1. Plankton Size Spectra

The compiled samples spanned substantial environmental variability across a variety of ocean domains (e.g., Longhurst, 2010). Surface chlorophyll *a* varied by more than two orders of magnitude (from 0.04 μg chl L^{-1} on HOT cruise 201 to 5.8 μg chl L^{-1} in a coastal upwelling region in the CCE). Vertically integrated NPP ranged from 14.5 to 364.3 mmol C m^{-2} day^{-1}. Notably, both the highest and lowest NPP rates were observed in regions of the CCE. Intraregional variability was reasonably low in the CRD, GoM, and HOT datasets, all of which had relatively warm surface temperatures and low surface chlorophyll. Variability was greater in the SalpPOOP dataset, which sampled both subtropical- and subantarctic-influenced waters of the Southern Ocean subtropical front (where chlorophyll *a* concentrations were generally higher in subtropical-influenced frontal waters), and in the CCE dataset, which sampled across a broad trophic gradient from coastal upwelling regions to oligotrophic waters, more representative of the North Pacific Subtropical Gyre.

Across this diverse dataset, the slope of the NBSS was relatively consistent, varying from −1.61 to −1.16 with an interquartile range of −1.44 to −1.32 (Figure 3, Figures S1–S3 in Supporting Information S1 and Table S2). For

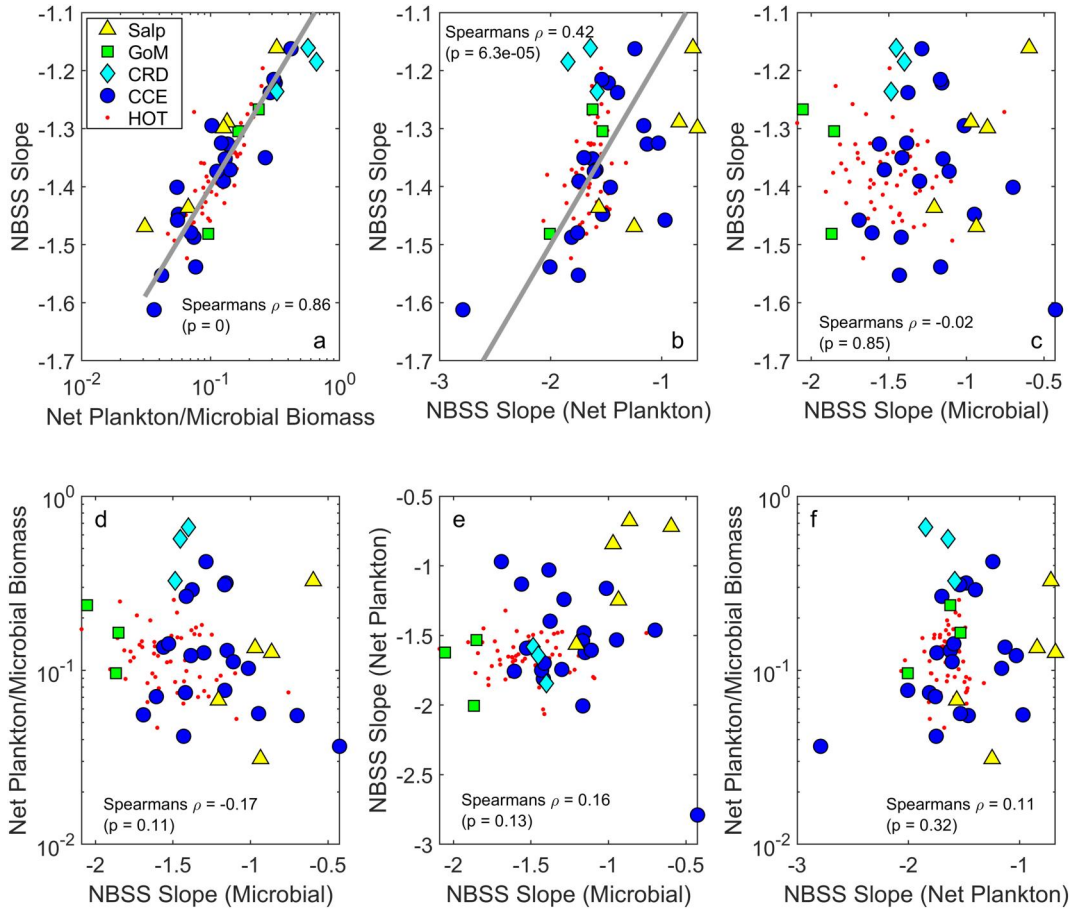

Figure 3. Relations between the overall Normalized Biomass Size Spectrum (NBSS) slope and different components of this slope including the ratio of net plankton (>200 μm) to microbial (<200 μm) carbon biomass, the NBSS slope of only the microbial portion of the size spectrum and the NBSS slope of only the net plankton portion of the size spectrum. Geometric mean linear regressions are plotted if the Spearman's rank correlation was significant ($p < 0.05$).

perspective, a NBSS slope of −1 implies equal biomass in logarithmically spaced size bins (e.g., biomass of small 1–10 μm organisms is the same as biomass of large 1–10 mm organisms). The consistent negative slope of the NBSS across all datasets suggests that (within the sampling size range of our methods, which is approximately 0.5 μm–10 mm) community biomass generally declines with increasing size. The median NBSS slope in our dataset (−1.37) equates to large 1–10 mm organisms having a biomass equal to only 7.6% of the biomass of small 1–10 μm organisms. The NBSS slope showed substantial variability across all of the regions sampled in our dataset, except for the CRD, which had a uniformly (relatively) high NBSS slope of ∼−1.2 across the three Lagrangian experiments conducted in the region (Figure 3).

The NBSS is, of course, driven by changes in the relative biomass of different size classes of organisms. To investigate in greater granularity how changes in size across the broad range of plankton sampled affects the overall NBSS slope, we also computed the NBSS slope for microbial taxa only (<200 μm, primarily including heterotrophic bacteria, phytoplankton, and heterotrophic protists), the NBSS slope for net plankton only (>200 μm, primarily metazoan zooplankton), and the ratio of net plankton biomass to microbial biomass (Figure 3). The ratio of net plankton biomass to microbial biomass varied from 0.031 to 0.66 and was strongly correlated with the NBSS slope (Spearman's $\rho = 0.86$, $p \ll 10^{-4}$, Figure 3a), implying that this ratio drives much of the variability in the NBSS slope. The slopes of the microbial and net plankton portions of the NBSS exhibited greater variability than the overall NBSS (−2.1 to −0.43 for the microbial portion; −2.8 to −0.68 for the net plankton portion). The slope of the net plankton NBSS was positively correlated with the slope of the overall NBSS ($\rho = 0.42$, $p < 10^{-4}$, Figure 3b). The slope of the microbial NBSS was uncorrelated with the slope of the overall NBSS (Figure 3c). This lack of correlation might seem surprising. However, it arises largely because

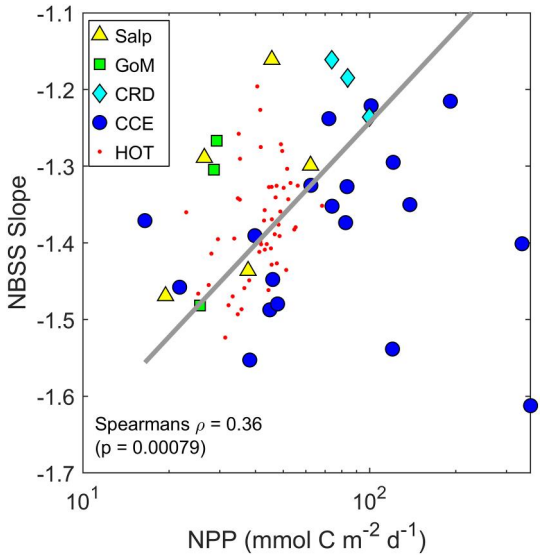

Figure 4. Relationship between the slope of the Normalized Biomass Size Spectrum (NBSS) and net primary production. Symbols are the same as Figure 3.

dominance by large phytoplankton was typically accompanied by a slight decrease in the ratio of net plankton to microbial biomass (Figure 3d).

The slopes of the microbial and net plankton portions of the NBSS and the ratio of net plankton to microbial biomass showed only weak and non-significant correlations with each other (Figures 3d–3f). These results were unexpected but likely reflect the complexity of ecological relationships among components of the plankton community.

We further compared the relationship between NPP and the slope of the NBSS to investigate the relationship between system productivity and plankton size spectra. We found a positive correlation ($\rho = 0.36$, $p < 10^{-3}$, Figure 4) despite the fact that the coastal CCE Lagrangian experiment with the highest NPP (voyage CCEP0605, cycle 3) also had the most negative NBSS slope. This relationship was also positive when comparing the slope of only the microbial portion of the NBSS to NPP (Figure S4a in Supporting Information S1) but did not exist when comparing the slope of the net plankton NBSS to NPP (Figure S4b in Supporting Information S1).

3.2. Carbon Export

Sinking carbon flux across the base of the euphotic zone was highly variable in the dataset, ranging from 1.2 to 52.2 mmol C m^{-2} day^{-1}. The lowest flux was measured at Station ALOHA and the highest flux was measured in the CCE, although carbon export was highly variable across the trophic gradient within the CCE. Carbon export strongly covaried with NPP (Spearman's $\rho = 0.51$, $p \ll 10^{-4}$). The Type II geometric mean regression relating export and NPP was: $\log_{10}(\text{Export}) = m \times \log_{10}(\text{NPP}) + b$, where $m = 1.85 \pm 0.17$ and $b = -2.55 \pm 0.29$ (Figure 5). Interregional variability in this relationship existed, with the CCE, GoM, and SalpPOOP Subtropical Front samples generally having greater than expected export relative to NPP and Station ALOHA and CRD having lower than expected export. Carbon export efficiency (ratio of carbon export to NPP) varied from 2.8% (on a HOT cruise at Station ALOHA) to 46.5% (for a salp bloom on the subantarctic edge of the Subtropical Front, east of New Zealand).

Carbon export was positively correlated with the slope of the NBSS (Spearman's $\rho = 0.34$, $p < 10^{-2}$), with a geometric mean regression of: $\log_{10}(\text{Export}) = m \times \log_{10}(\text{NBSS}_{\text{Slope}}) + b$, where $m = 3.88 \pm 0.52$ and $b = 5.82 \pm 0.72$ (Figure 6a). Carbon export also had positive relationships with the NBSS slope of the microbial portion of the size spectrum (Spearman's $\rho = 0.35$, $p < 10^{-2}$, Figure S5a in Supporting Information S1) and with the ratio of net plankton to microbial biomass (Spearman's $\rho = 0.31$, $p < 10^{-2}$, Figure S5c in Supporting Information S1). However, export was not significantly related to the NBSS slope of the net plankton portion of the size spectrum (Figure S5b in Supporting Information S1). This suggests that larger phytoplankton sizes and increased relative biomass of mesozooplankton lead to higher carbon exports, but that mesozooplankton size does not drive export rates. Carbon export efficiency was not statistically related to the NBSS slope (Figure 6b), indicating that plankton size does not have a strong relationship with the proportion of phytoplankton production that is exported from the surface ocean.

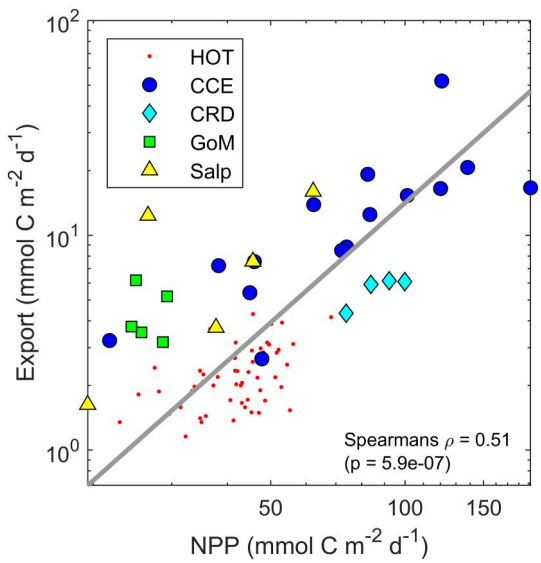

Figure 5. Relationship between sinking organic carbon flux (at the base of the euphotic zone) and net primary production.

To further investigate the relationships among carbon export, size spectra, and other environmental factors, we used LASSO regression. Independent variables considered in the model were: slopes of the overall, microbial and net plankton portions of the NBSS, log-transformed ratios of net plankton to microbial biomass, log-transformed rates of NPP, log-transformed surface chlorophyll *a* (Chl), and sea-surface temperature (SST). The latter three factors were chosen because they are commonly used predictors of sinking particle flux (e.g., Dunne et al., 2005; Laws et al., 2011). The dependent

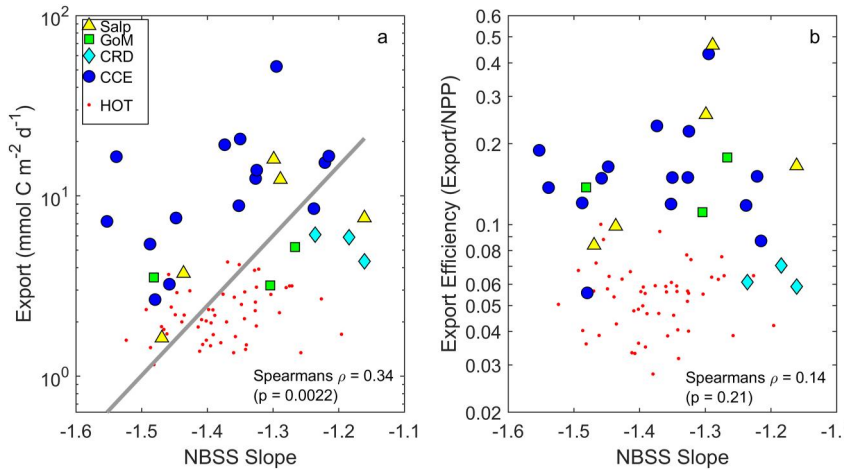

Figure 6. Relationship between the Normalized Biomass Size Spectrum (NBSS) slope and sinking carbon export at the base of the euphotic zone (a) and carbon export efficiency (export/net primary production, b).

variable was log-transformed carbon export. At the commonly used λ threshold of minimum squared error plus one standard error, LASSO parameter selection suggested that only NPP, surface chlorophyll *a*, and SST were useful predictive parameters, with an equation of: $\log_{10}(\text{Export}) = 0.54 \times \log_{10}(\text{NPP}) + 0.24 \times \log_{10}(\text{Chl}) - 0.013 \times \text{SST} + 0.11$. This suggests that knowledge of the plankton size spectrum does not add informative power relative to other more easily measured ecosystem or physical metrics. Interestingly, when we use a weaker threshold for λ (minimum squared error), the model also included the NBSS slope of the net plankton portion of the size spectrum and the ratio of net plankton to microbial biomass (both with positive coefficients). This suggests that, if all else is equal, increased zooplankton size and biomass is associated with higher exports. We caution, however, that while this lower λ threshold is sometimes utilized, it is prone to overfitting of the data. Given the very limited range of environmental variability for HOT samples, which comprised a large portion of our dataset, we also considered a LASSO regression model that excluded HOT data (again defaulting to the commonly used λ threshold of minimum squared error plus one standard error). Results included only NPP and surface chlorophyll as predictors with a model represented by $\log_{10}(\text{Export}) = 0.25 \times \log_{10}(\text{NPP}) + 0.16 \log_{10}(\text{Chl}) + 0.51$.

4. Discussion

As a result of the numerous ways in which organismal physiology and ecology are related to size (Beardall et al., 2009; Branco et al., 2020; Hansen et al., 1997; Marañón, 2015), plankton size spectra are a potentially useful emergent property of pelagic ecosystems. Indeed, multiple studies have identified coherent patterns in plankton size. Latitudinal patterns suggest that mean phytoplankton cell size and cell size diversity increase in colder regions (Acevedo-Trejos et al., 2018; Kostadinov et al., 2010), while patterns from the tropical and subtropical Pacific show increasing phytoplankton size with nutrient loading (Goericke, 2011; Taylor & Landry, 2018). Taken together, these results suggest that the competitive dominance of small cells under nutrient-depleted conditions may be an important driver of plankton size spectra (Edwards et al., 2012). Alternate explanations, however, focus on competition-neutral explanations related to grazing or community dilution processes in stable or temporally variable environments (Behrenfeld et al., 2021). A similar pattern of decreased size in warmer and less productive ecosystems has been found for metazoan zooplankton (Brandão et al., 2021; Rykaczewski, 2019), although results from a circumglobal project found relatively little spatial variability in zooplankton size spectral slopes (Mompean et al., 2016). Similarly, Décima (2022) found greater relative dominance by large zooplankton in the oligotrophic North Pacific Subtropical Gyre than in a coastal upwelling biome.

While these and other studies have investigated phytoplankton or zooplankton size spectra separately, few have quantified size spectra across the μm to cm range required to fully characterize plankton communities. Investigation of particle size spectra across these size ranges suggests that most particle mass in plankton assemblages is in the 0.1–3 mm size range, although most of the particles assessed were likely non-living detritus (Jackson et al., 1997). A recent global compilation of living organisms suggests a relatively flat marine size spectrum from

bacteria to whales but sheds little light on variability in this extremely broad size spectrum (Hatton et al., 2021). San Martin, Irigoien, et al. (2006) found no relationship between the size spectral slopes and total plankton biomass along a north-south transect in the Atlantic Ocean and concluded that trophic transfer efficiency was not increased in more productive regions. Similarly, no distinct differences in size spectra were found in the two regions of the northwest Atlantic (Quiñones et al., 2003). These results contrast with the results of multiple modeling studies that consistently predict shallower size spectral slopes in productive regions (Fuchs & Franks, 2010; Negrete-García et al., 2022; Ward et al., 2012).

The range of results found above may derive from the inherent spatiotemporal variability that exists in plankton communities at multiple spatial and temporal scales. However, it may also reflect methodological differences among investigators, which highlights the importance of internal consistency when investigating the relationships between size spectra and environmental variables. Across the five regions included in our synthesis, we find that the NBSS slopes vary from −1.61 to −1.16 with a mean of −1.37. These slopes are slightly steeper than the average of −1.14 found by Quiñones et al. (2003) for the Sargasso Sea and New England Seamounts regions or by San Martin, Harris, and Irigoien (2006) on the Atlantic meridional transect (regional averages varying from −1.29 to −0.99). Our results are also consistently steeper than the overall negative one slope predicted by Sheldon et al. (1972). It is possible that our slopes are slightly biased toward negative values as a result of net avoidance by the largest (and hence strongest swimming) zooplankton. We explicitly considered our largest size class to encompass 5–50 mm organisms, although many cm-sized organisms (e.g., euphausiids) are likely capable of net avoidance, particularly during the day, and this size class includes not only zooplankton but also some micronekton. If we exclude this largest size class, the NBSS slope varies from −1.47 to −1.01 with a mean of −1.29. The slopes of the full size spectra were highly correlated with the slopes of the size spectra excluding the largest size class (Pearson's $\rho = 0.85, p \ll 10^{-6}$). If the largest size class is excluded from the NBSS slope, the correlation between NPP and NBSS slope remains virtually unchanged although the correlation between NBSS slope and export decreases from 0.34 to 0.18. This suggests that while potential net avoidance by zooplankton may lead to a slight underestimate of NBSS slopes, it does not substantially change our conclusions that NBSS slope is only weakly predictive of export efficiency. Escapement can also lead to an under-collection bias in the smallest zooplankton size class, although sensitivity analyses show that exclusion of this size class has negligible impacts on the computed size spectra.

Our results are derived from labor-intensive net tow, microscopy, and flow cytometry measurements that provide relatively coarse size resolution. In contrast, autonomous and tethered in situ imaging approaches allow rapid throughput and high-resolution size spectral analyses (Dugenne et al., 2023; Orenstein et al., 2022; Stemmann & Boss, 2011). For instance, the Imaging Flowcytobot is frequently used for near-continuous measurements of surface phytoplankton (∼10–100 μm) communities at either single stations or in ship flowthrough seawater systems during transit (Olson & Sosik, 2007); the underwater vision profiler can be used to rapidly image zooplankton (∼0.6–3 mm) communities during CTD-Niskin rosette vertical profiles (Picheral et al., 2010); and the In Situ Ichthyoplankton Imaging System is optimized for imaging larger zooplankton (∼1–20 mm) during undulating towed deployments (Cowen et al., 2013). These approaches offer several advantages including rapid data collection and the measurement of additional organism characteristics, such as opacity. However, they are arguably less accurate for the current application, because they rely on conversions from cross-sectional area to carbon contents, which can vary substantially between taxa and are often orientation-dependent. The present dataset, while limited to approximately octave-scale size resolution, is likely more robust for comparing size spectral changes across several order-of-magnitude differences in organismal size to independently measured ecosystem properties.

By investigating relationships amongst different portions of the community, we found that the whole community NBSS slope was strongly positively correlated with the net plankton to microbial biomass ratio (Figure 3a) and the NBSS slope of the net plankton (Figure 3c) but not correlated with the NBSS slope of the microbial community (Figure 3b). These results are in general agreement with the findings of San Martin, Irigoien, et al. (2006), who found that the whole community NBSS slope was positively correlated to mesoplankton (i.e., our net plankton, >200 μm) biomass but not to the ratio of picoplankton to microplankton biomass (i.e., a metric related to the NBSS slope of microbial communities). We also found a weak (and not statistically significant) negative relationship between the NBSS slope of microbial communities and the ratio of net plankton to microbial biomass (Figure 3d). This relationship likely relates to the relationship between the percentage contribution of large phytoplankton and total phytoplankton biomass that has been noted in previous studies (Chisholm, 1992;

Goericke, 2011). When phytoplankton biomass is high, large phytoplankton biomass increases and simultaneously the ratio of zooplankton tophytoplankton is likely to be lower because such high phytoplankton biomass is in the denominator.

Our findings bolster previous results suggesting that the communities in productive regions are dominated disproportionately by large plankton (e.g., Acevedo-Trejos et al., 2018; Brandão et al., 2021; Taylor & Landry, 2018), but they also add nuance to these conclusions. We found reasonably strong positive correlations between NPP and the whole community NBSS slope (Spearman's $\rho = 0.36$, $p < 0.001$, Figure 4) and the microbial community NBSS slope (Spearman's $\rho = 0.39$, $p < 0.001$, Figure S4a in Supporting Information S1), while the ratio of net plankton to microbial biomass was weaker (Spearman's $\rho = 0.29$, $p = 0.007$, Figure S4c in Supporting Information S1). There was no statistically significant relationship between the NBSS slope for net plankton and NPP, suggesting that zooplankton size is not related to NPP, in contrast to the results from Brandão et al. (2021). The Brandão et al. (2021) study, which compiled results from the global Tara Expedition, featured a strong correlation between temperature and metrics of ecosystem productivity (e.g., chlorophyll *a* concentration), suggesting the possibility that their results may indicate the importance of temperature as an underlying driver of zooplankton size rather than productivity. Relationships between ecosystem productivity and plankton size spectra are also affected by the inherent lag times associated with biological production. In our study regions, phytoplankton responses to favorable growth conditions will occur within a time span of a day to a week. However, zooplankton blooms develop over longer and highly variable durations that can range from days to months depending on taxa, temperature, and species-specific phenological patterns (Almén & Tamelander, 2020; Riegman et al., 1993). These lags can thus obscure relationships between plankton size spectra and other ecosystem metrics, particularly in cold regions with slow-growing taxa. Nevertheless, the positive correlation between NPP and the ratio of net plankton to microbial biomass (Figure S4c in Supporting Information S1) suggests increased ecosystem transfer efficiency in productive ecosystems, in agreement with prior studies (e.g., Hunt et al., 2015; Stock & Dunne, 2010).

Our results provide more equivocal support for the relationship between plankton size spectra and the BCP. Previous studies relating carbon export to plankton size have mostly focused on phytoplankton size (Boyd & Newton, 1999; Buesseler & Boyd, 2009; Mouw et al., 2016; Siegel et al., 2014). Such studies typically find high export when communities are dominated by large phytoplankton, especially diatoms (Cai et al., 2015; Krause et al., 2015; Smetacek et al., 2012). Regions dominated by cyanobacteria and picoeukaryotes typically have lower export (Karl & Church, 2014; Lomas & Moran, 2011; Stukel et al., 2013). Despite this focus on phytoplankton, a global synthesis by Henson et al. (2019) suggests the importance of evaluating entire plankton community dynamics for understanding sinking carbon flux. Using a size-structured plankton ecosystem model, Serra-Pompei et al. (2022) also found that carbon export efficiency (sinking flux/NPP) was more closely related to the slope of the NBSS (referred to as λ in their model) than to other characteristics of the community. Our results clearly suggest that carbon export is higher in regions dominated by larger plankton (Spearman's $\rho = 0.34$, $p = 0.002$, Figure 6a). However, we did not find a statistically significant correlation between export efficiency and the NBSS slope (although the non-significant correlation was positive, as predicted, Figure 6b). Our results also align with a recent study from the Sargasso Sea showing that zooplankton size did not correlate with export flux (Perhirin et al., 2024). That study also showed that opacity was an important zooplankton trait that correlated strongly with export flux, and although we could not quantify opacity from our dataset, several of our highest export efficiency locations (from the SalpPOOP cruise, Décima et al., 2023) were measured within a bloom of highly transparent pelagic tunicates. We further note that our sinking particle measurements do not include the potential impact of zooplankton carcasses, which can be substantial in some regions (Frangoulis et al., 2011; Halfter et al., 2022; Smith et al., 2014) and would covary with abundance of large taxa. Despite this caveat, it is striking that when conducting LASSO regression to ascertain the ecosystem characteristics that were useful predictors of carbon export, SST, sea-surface chlorophyll *a*, and NPP were all significant predictors, but none of the parameters associated with the size spectrum were significant. This suggests that while export and export efficiency are in fact higher when the community is dominated by large organisms, it is not the presence of large organisms that necessarily drives the high exports. Instead, plankton size and the strength of the BCP may respond similarly to other underlying ecosystem properties.

5. Conclusions

Plankton size spectra are an emergent property of pelagic ecosystems that derives from the myriad ways in which ecophysiological parameters correlate with organism size. In this study, we compiled the largest internally

consistent database across a range of oceanic domains including collocated (in time and space) measurements of plankton ecosystem size spectra, NPP, and carbon export. We found strong positive correlations between NPP and the whole ecosystem size spectrum, the size spectrum of microbial communities, and the ratio of net plankton (mostly zooplankton) to microbial community (protists and bacteria) biomass. These all illustrate that community size shifts toward larger organisms in more productive times and places, with implications for ecosystem trophic efficiency. However, we did not find a correlation between the size of net-collected zooplankton and NPP, which suggests that other ecological processes occurring within the zooplankton community are at least as important as phytoplankton production in determining the size spectra of metazoan zooplankton. Our results further show that sinking-particle carbon export is positively correlated with whole community size spectra, but that size spectra provide no additional explanatory power for predicting carbon export relative to other commonly used metrics (NPP, sea-surface chlorophyll, and SST).

Data Availability Statement

Data used in this study are available through the open repositories Biological and Chemical Oceanography Data Management Office (BCO-DMO) and Environmental Data Initiative (EDI). Specifically, CCE data are available on CCE LTER Datazoo (https://oceaninformatics.ucsd.edu/datazoo/catalogs/ccelter/datasets) and are also archived at EDI (https://portal.edirepository.org/). SalpPOOP data are available at https://www.bco-dmo.org/project/754878. BLOOFINZ-GoM data are available at https://www.bco-dmo.org/project/834957. CRD data are available at https://www.bco-dmo.org/project/515387. HOT data are available through BCO-DMO (https://www.bco-dmo.org/project/2101) and the HOT website (https://hahana.soest.hawaii.edu/hot/). Our compiled size spectrum data are available as supplementary tables in this manuscript and have also been submitted to BCO-DMO under the SalpPOOP landing page.

Acknowledgments

We would like to thank our many collaborators in the CCE LTER, BLOOFINZ, SalpPOOP, and CRD FluZIE projects. We are also grateful to the many researchers in the Hawaii Ocean Time-series (HOT) program for their dedication to providing high quality and freely available data. This research was supported by National Science Foundation Grants OCE-2224726 to the CCE LTER Program, OCE-1756517 to HOT, OCE-1756610 and OCE-1851347 to M.R.S., OCE-1756465 to K.E.S., and OCE-0826626 to M.R.L. It was also supported by the National Oceanic and Atmospheric Administration's RESTORE Program Grant (Project Title: Effects of nitrogen sources and plankton food-web dynamics on habitat quality for the larvae of ABT in the GoM; under federal funding opportunity NOAA-NOSNCCOS-2017-2004875). Additional funding was provided by a Royal Society of New Zealand Marsden Fast-track award to M.D. and Strategic Science Investment Fund and Tangaroa Reference Group vessel funding from the New Zealand Ministry of Business, Innovation and Employment to National Center—Coasts & Oceans (NIWA) for the SalpPOOP voyage and sample analyses to M.D. and S.D.N.

References

Acevedo-Trejos, E., Marañón, E., & Merico, A. (2018). Phytoplankton size diversity and ecosystem function relationships across oceanic regions. *Proceedings of the Royal Society B: Biological Sciences*, *285*(1879), 20180621. https://doi.org/10.1098/rspb.2018.0621

Alldredge, A. L., & Gotschalk, C. C. (1989). Direct observations of the mass flocculation of diatom blooms: Characteristics, settling velocities and formation of diatom aggregates. *Deep-Sea Research*, *36*(2), 159–171. https://doi.org/10.1016/0198-0149(89)90131-3

Almén, A.-K., & Tamelander, T. (2020). Temperature-related timing of the spring bloom and match between phytoplankton and zooplankton. *Marine Biology Research*, *16*(8–9), 674–682. https://doi.org/10.1080/17451000.2020.1846201

Archibald, K. M., Siegel, D. A., & Doney, S. C. (2019). Modeling the impact of zooplankton diel vertical migration on the carbon export flux of the biological pump. *Global Biogeochemical Cycles*, *33*(2), 181–199. https://doi.org/10.1029/2018gb005983

Beardall, J., Allen, D., Bragg, J., Finkel, Z. V., Flynn, K. J., Quigg, A., et al. (2009). Allometry and stoichiometry of unicellular, colonial and multicellular phytoplankton. *New Phytologist*, *181*(2), 295–309. https://doi.org/10.1111/j.1469-8137.2008.02660.x

Behrenfeld, M. J., Boss, E. S., & Halsey, K. H. (2021). Phytoplankton community structuring and succession in a competition-neutral resource landscape. *ISME Communications*, *1*, 1–8. https://doi.org/10.1038/s43705-021-00011-5

Boyd, P. W., Claustre, H., Levy, M., Siegel, D. A., & Weber, T. (2019). Multi-faceted particle pumps drive carbon sequestration in the ocean. *Nature*, *568*(7752), 327–335. https://doi.org/10.1038/s41586-019-1098-2

Boyd, P. W., & Newton, P. (1999). Does planktonic community structure determine downward particulate organic carbon flux in different oceanic provinces? *Deep-Sea Research I*, *46*(1), 63–91. https://doi.org/10.1016/s0967-0637(98)00066-1

Branco, P., Egas, M., Hall, S. R., & Huisman, J. (2020). Why do phytoplankton evolve large size in response to grazing? *The American Naturalist*, *195*(1), E20–E37. https://doi.org/10.1086/706251

Brandão, M. C., Benedetti, F., Martini, S., Soviadan, Y. D., Irisson, J. O., Romagnan, J. B., et al. (2021). Macroscale patterns of oceanic zooplankton composition and size structure. *Scientific Reports*, *11*, 1–19. https://doi.org/10.1038/s41598-021-94615-5

Buesseler, K. O., & Boyd, P. W. (2009). Shedding light on processes that control particle export and flux attenuation in the twilight zone of the open ocean. *Limnology & Oceanography*, *54*(4), 1210–1232. https://doi.org/10.4319/lo.2009.54.4.1210

Burd, A., Buchan, A., Church, M., Landry, M., McDonnell, A., Passow, U., et al. (2016). Towards a transformative understanding of the ocean's biological pump: Priorities for future research. Report of the NSF Biology of the Biological Pump Workshop, Feb. 19–20, 2016 (p. 36).

Cai, P., Zhao, D., Wang, L., Huang, B., & Dai, M. (2015). Role of particle stock and phytoplankton community structure in regulating particulate organic carbon export in a large marginal sea. *Journal of Geophysical Research: Oceans*, *120*(3), 2063–2095. https://doi.org/10.1002/2014jc010432

Carlson, C. A., Ducklow, H. W., & Michaels, A. F. (1994). Annual flux of dissolved organic carbon from the euphotic zone in the northwestern Sargasso Sea. *Nature*, *371*(6496), 405–408. https://doi.org/10.1038/371405a0

Chisholm, S. W. (1992). Phytoplankton size. In *Primary productivity and biogeochemical cycles in the sea* (pp. 213–237).

Church, M. J., Lomas, M. W., & Muller-Karger, F. (2013). Sea change: Charting the course for biogeochemical ocean time-series research in a new millennium. *Deep-Sea Research II*, *93*, 2–15. https://doi.org/10.1016/j.dsr2.2013.01.035

Cowen, R. K., Greer, A. T., Guigand, C. M., Hare, J. A., Richardson, D. E., & Walsh, H. J. (2013). Evaluation of the In Situ Ichthyoplankton Imaging System (ISIIS): Comparison with the traditional (bongo net) sampler. *Fishery Bulletin*, *111*, 1–12. https://doi.org/10.7755/fb.111.1.1

Décima, M. (2022). Zooplankton trophic structure and ecosystem productivity. *Marine Ecology Progress Series*, *692*, 23–42. https://doi.org/10.3354/meps14077

Décima, M., Landry, M. R., Stukel, M. R., Lopez-Lopez, L., & Krause, J. W. (2016). Mesozooplankton biomass and grazing in the Costa Rica Dome: Amplifying variability through the plankton food web. *Journal of Plankton Research*, *38*(2), 317–330. https://doi.org/10.1093/plankt/fbv091

Décima, M., Stukel, M. R., Nodder, S. D., Gutiérrez-Rodríguez, A., Selph, K. E., dos Santos, A. L., et al. (2023). Salp blooms drive strong increases in passive carbon export in the Southern Ocean. *Nature Communications*, *14*(1), 425. https://doi.org/10.1038/s41467-022-35204-6

Ducklow, H. W., Steinberg, D. K., & Buesseler, K. O. (2001). Upper ocean carbon export and the biological pump. *Oceanography*, *14*(4), 50–58. https://doi.org/10.5670/oceanog.2001.06

Dugenne, M., Corrales-Ugalde, M., Luo, J., Kiko, R., O'Brien, T., Irsison, J.-O., et al. (2023). First release of the Pelagic Size Structure database: Global datasets of marine size spectra obtained from plankton imaging devices. *Earth System Science Data Discussions*, *2023*, 1–41.

Dunne, J. P., Armstrong, R. A., Gnanadesikan, A., & Sarmiento, J. L. (2005). Empirical and mechanistic models for the particle export ratio. *Global Biogeochemical Cycles*, *19*(4), GB4026. https://doi.org/10.1029/2004gb002390

Edwards, K. F., Thomas, M. K., Klausmeier, C. A., & Litchman, E. (2012). Allometric scaling and taxonomic variation in nutrient utilization traits and maximum growth rate of phytoplankton. *Limnology & Oceanography*, *57*(2), 554–566. https://doi.org/10.4319/lo.2012.57.2.0554

Frangoulis, C., Skliris, N., Lepoint, G., Elkalay, K., Goffart, A., Pinnegar, J. K., & Hecq, J. H. (2011). Importance of copepod carcasses versus faecal pellets in the upper water column of an oligotrophic area. *Estuarine, Coastal and Shelf Science*, *92*(3), 456–463. https://doi.org/10.1016/j.ecss.2011.02.005

Fry, B., & Quiñones, R. B. (1994). Biomass spectra and stable isotope indicators of trophic level in zooplankton of the northwest Atlantic. *Marine Ecology Progress Series*, *112*, 201–204. https://doi.org/10.3354/meps112201

Fuchs, H. L., & Franks, P. J. S. (2010). Plankton community properties determined by nutrients and size-selective feeding. *Marine Ecology Progress Series*, *413*, 1–15. https://doi.org/10.3354/meps08716

Gerard, T., Lamkin, J. T., Kelly, T. B., Knapp, A. N., Laiz-Carrión, R., Malca, E., et al. (2022). Bluefin larvae in oligotrophic ocean foodwebs, investigations of nutrients to zooplankton: Overview of the BLOOFINZ-Gulf of Mexico program. *Journal of Plankton Research*, *44*(5), 600–617. https://doi.org/10.1093/plankt/fbac038

Goericke, R. (2011). The size structure of marine phytoplankton - What are the rules? *California Cooperative Oceanic Fisheries Investigations Reports*, *52*, 198–204.

Gutierrez-Rodriguez, A., Stukel, M. R., Lopes dos Santos, A., Biard, T., Scharek, R., Vaulot, D., et al. (2019). High contribution of Rhizaria (Radiolaria) to vertical export in the California Current Ecosystem revealed by DNA metabarcoding. *ISME Journal*, *13*(4), 964–976. https://doi.org/10.1038/s41396-018-0322-7

Halfter, S., Cavan, E. L., Butterworth, P., Swadling, K. M., & Boyd, P. W. (2022). "Sinking dead"—How zooplankton carcasses contribute to particulate organic carbon flux in the subantarctic Southern Ocean. *Limnology & Oceanography*, *67*(1), 13–25. https://doi.org/10.1002/lno.11971

Hansen, P. J., Bjornsen, P. K., & Hansen, B. W. (1997). Zooplankton grazing and growth: Scaling within the 2-2,000-mu m body size range. *Limnology & Oceanography*, *42*(4), 687–704. https://doi.org/10.4319/lo.1997.42.4.0687

Hatton, I. A., Heneghan, R. F., Bar-On, Y. M., & Galbraith, E. D. (2021). The global ocean size spectrum from bacteria to whales. *Science Advances*, *7*(46), eabh3732. https://doi.org/10.1126/sciadv.abh3732

Henson, S. A., Laufkötter, C., Leung, S., Giering, S. L. C., Palevsky, H. I., & Cavan, E. L. (2022). Uncertain response of ocean biological carbon export in a changing world. *Nature Geoscience*, *15*(4), 248–254. https://doi.org/10.1038/s41561-022-00927-0

Henson, S. A., Le Moigne, F., & Giering, S. (2019). Drivers of carbon export efficiency in the global ocean. *Global Biogeochemical Cycles*, *33*(7), 891–903. https://doi.org/10.1029/2018gb006158

Hunt, B. P., Allain, V., Menkes, C., Lorrain, A., Graham, B., Rodier, M., et al. (2015). A coupled stable isotope-size spectrum approach to understanding pelagic food-web dynamics: A case study from the southwest sub-tropical Pacific. *Deep-Sea Research II*, *113*, 208–224. https://doi.org/10.1016/j.dsr2.2014.10.023

Iguchi, N., & Ikeda, T. (2004). Metabolism and elemental composition of aggregate and solitary forms of *Salpa thompsoni* (Tunicata: Thaliacea) in waters off the Antarctic Peninsula during austral summer 1999. *Journal of Plankton Research*, *26*(9), 1025–1037. https://doi.org/10.1093/plankt/fbh093

Jackson, G. A., Maffione, R., Costello, D. K., Alldredge, A. L., Logan, B. E., & Dam, H. G. (1997). Particle size spectra between 1 μm and 1 cm at Monterey Bay determined using multiple instruments. *Deep-Sea Research I*, *44*(11), 1739–1767. https://doi.org/10.1016/s0967-0637(97)00029-0

Jackson, G. A., Waite, A. M., & Boyd, P. W. (2005). Role of algal aggregation in vertical carbon export during SOIREE and in other low biomass environments. *Geophysical Research Letters*, *32*(13), 4. https://doi.org/10.1029/2005gl023180

Karl, D. M., Christian, J., Dore, J., Hebel, D., Letelier, R., Tupas, L., & Winn, C. (1996). Seasonal and interannual variability in primary production and particle flux at Station ALOHA. *Deep-Sea Research II*, *43*(2–3), 539–568. https://doi.org/10.1016/0967-0645(96)00002-1

Karl, D. M., & Church, M. J. (2014). Microbial oceanography and the Hawaii Ocean Time-series programme. *Nature Reviews Microbiology*, *12*(10), 699–713. https://doi.org/10.1038/nrmicro3333

Kellogg, C. T. E., Carpenter, S. D., Renfro, A. A., Sallon, A., Michel, C., Cochran, J. K., & Deming, J. W. (2011). Evidence for microbial attenuation of particle flux in the Amundsen Gulf and Beaufort Sea: Elevated hydrolytic enzyme activity on sinking aggregates. *Polar Biology*, *34*(12), 2007–2023. https://doi.org/10.1007/s00300-011-1015-0

Knauer, G. A., Martin, J. H., & Bruland, K. W. (1979). Fluxes of particulate carbon, nitrogen, and phosphorus in the upper water column of the Northeast Pacific. *Deep-Sea Research*, *26*(1), 97–108. https://doi.org/10.1016/0198-0149(79)90089-x

Kostadinov, T. S., Siegel, D. A., & Maritorena, S. (2010). Global variability of phytoplankton functional types from space: Assessment via the particle size distribution. *Biogeosciences*, *7*(10), 3239–3257. https://doi.org/10.5194/bg-7-3239-2010

Krause, J. W., Brzezinski, M. A., Goericke, R., Landry, M. R., Ohman, M. D., Stukel, M. R., & Taylor, A. G. (2015). Variability in diatom contributions to biomass, organic matter production and export across a frontal gradient in the California Current Ecosystem. *Journal of Geophysical Research: Oceans*, *120*(2), 1032–1047. https://doi.org/10.1002/2014jc010472

Landry, M. R. (2009). Grazing processes and secondary production in the Arabian Sea: A simple food web synthesis with measurement constraints. In J. D. Wiggert, R. R. Hood, S. W. A. Naqvi, K. H. Brink, & S. L. Smith (Eds.), *Indian Ocean biogeochemical processes and ecological variability*, *AGU Monograph* (pp. 133–146). American Geophysical Union.

Landry, M. R., Al-Mutairi, H., Selph, K. E., Christensen, S., & Nunnery, S. (2001). Seasonal patterns of mesozooplankton abundance and biomass at Station ALOHA. *Deep-Sea Research II*, *48*(8–9), 2037–2061. https://doi.org/10.1016/s0967-0645(00)00172-7

Landry, M. R., De Verneil, A., Goes, J. I., & Moffett, J. W. (2016). Plankton dynamics and biogeochemical fluxes in the Costa Rica Dome: Introduction to the CRD Flux and Zinc Experiments. *Journal of Plankton Research*, *38*(2), 167–182. https://doi.org/10.1093/plankt/fbv103

Landry, M. R., Ohman, M. D., Goericke, R., Stukel, M. R., & Tsyrklevich, K. (2009). Lagrangian studies of phytoplankton growth and grazing relationships in a coastal upwelling ecosystem off Southern California. *Progress in Oceanography*, *83*(1–4), 208–216. https://doi.org/10.1016/j.pocean.2009.07.026

Landry, M. R., & Swalethorp, R. (2021). Mesozooplankton biomass, grazing and trophic structure in the Bluefin tuna spawning area of the oceanic Gulf of Mexico. *Journal of Plankton Research*, *44*(5), 677–691. https://doi.org/10.1093/plankt/fbab008

Laws, E. A., D'Sa, E., & Naik, P. (2011). Simple equations to estimate ratios of new or export production to total production from satellite-derived estimates of sea surface temperature and primary production. *Limnology & Oceanography: Methods*, *9*(12), 593–601. https://doi.org/10.4319/lom.2011.9.593

Levy, M., Bopp, L., Karleskind, P., Resplandy, L., Ethe, C., & Pinsard, F. (2013). Physical pathways for carbon transfers between the surface mixed layer and the ocean interior. *Global Biogeochemical Cycles*, *27*(4), 1001–1012. https://doi.org/10.1002/gbc.20092

Lomas, M. W., & Moran, S. B. (2011). Evidence for aggregation and export of cyanobacteria and nano-eukaryotes from the Sargasso Sea euphotic zone. *Biogeosciences*, *8*(1), 203–216. https://doi.org/10.5194/bg-8-203-2011

Longhurst, A. R. (2010). *Ecological geography of the sea*. Elsevier.

Longhurst, A. R., Bedo, A. W., Harrison, W. G., Head, E. J. H., & Sameoto, D. D. (1990). Vertical flux of respiratory carbon by oceanic diel migrant biota. *Deep-Sea Research*, *37*(4), 685–694. https://doi.org/10.1016/0198-0149(90)90098-g

Marañón, E. (2015). Cell size as a key determinant of phytoplankton metabolism and community structure. *Annual Review of Marine Science*, *7*(1), 241–264. https://doi.org/10.1146/annurev-marine-010814-015955

Martin, J. H., Knauer, G. A., Karl, D. M., & Broenkow, W. W. (1987). Vertex: Carbon cycling in the northeast Pacific. *Deep-Sea Research*, *34*(2), 267–285. https://doi.org/10.1016/0198-0149(87)90086-0

Menden-Deuer, S., & Lessard, E. J. (2000). Carbon to volume relationships for dinoflagellates, diatoms, and other protist plankton. *Limnology & Oceanography*, *45*(3), 569–579. https://doi.org/10.4319/lo.2000.45.3.0569

Michaels, A. F., & Silver, M. W. (1988). Primary production, sinking fluxes and the microbial food web. *Deep-Sea Research*, *35*(4), 473–490. https://doi.org/10.1016/0198-0149(88)90126-4

Mislan, K. A. S., Stock, C. A., Dunne, J. P., & Sarmiento, J. L. (2014). Group behavior among model bacteria influences particulate carbon remineralization depths. *Journal of Marine Research*, *72*(3), 183–218. https://doi.org/10.1357/002224014814901985

Mompean, C., Bode, A., Latasa, M., Fernández-Castro, B., Mouriño-Carballido, B., & Irigoien, X. (2016). The influence of nitrogen inputs on biomass and trophic structure of ocean plankton: A study using biomass and stable isotope size-spectra. *Journal of Plankton Research*, *38*(5), 1163–1177. https://doi.org/10.1093/plankt/fbw052

Morrow, R. M., Ohman, M. D., Goericke, R., Kelly, T. B., Stephens, B. M., & Stukel, M. R. (2018). Primary productivity, mesozooplankton grazing, and the biological pump in the California Current Ecosystem: Variability and response to El Niño. *Deep-Sea Research I*, *140*, 52–62. https://doi.org/10.1016/j.dsr.2018.07.012

Mouw, C. B., Barnett, A., McKinley, G. A., Gloege, L., & Pilcher, D. (2016). Global ocean particulate organic carbon flux merged with satellite parameters. *Earth System Science Data*, *8*(2), 531–541. https://doi.org/10.5194/essd-8-531-2016

Negrete-García, G., Luo, J. Y., Long, M. C., Lindsay, K., Levy, M., & Barton, A. D. (2022). Plankton energy flows using a global size-structured and trait-based model. *Progress in Oceanography*, *209*, 102898. https://doi.org/10.1016/j.pocean.2022.102898

Nowicki, M., DeVries, T., & Siegel, D. A. (2022). Quantifying the carbon export and sequestration pathways of the ocean's biological carbon pump. *Global Biogeochemical Cycles*, *36*(3), e2021GB007083. https://doi.org/10.1029/2021gb007083

Ohman, M. D., Barbeau, K., Franks, P. J. S., Goericke, R., Landry, M. R., & Miller, A. J. (2013). Ecological transitions in a coastal upwelling ecosystem. *Oceanography*, *26*(3), 210–219. https://doi.org/10.5670/oceanog.2013.65

Olson, R. J., & Sosik, H. M. (2007). A submersible imaging-in-flow instrument to analyze nano-and microplankton: Imaging FlowCytobot. *Limnology & Oceanography: Methods*, *5*(6), 195–203. https://doi.org/10.4319/lom.2007.5.195

Omand, M. M., D'Asaro, E. A., Lee, C. M., Perry, M. J., Briggs, N., Cetinić, I., & Mahadevan, A. (2015). Eddy-driven subduction exports particulate organic carbon from the spring bloom. *Science*, *348*(6231), 222–225. https://doi.org/10.1126/science.1260062

Orenstein, E. C., Ayata, S., Maps, F., Becker, É. C., Benedetti, F., Biard, T., et al. (2022). Machine learning techniques to characterize functional traits of plankton from image data. *Limnology & Oceanography*, *67*(8), 1647–1669. https://doi.org/10.1002/lno.12101

Pasulka, A. L., Landry, M. R., Taniguchi, D. A., Taylor, A. G., & Church, M. J. (2013). Temporal dynamics of phytoplankton and heterotrophic protists at station ALOHA. *Deep-Sea Research II*, *93*, 44–57. https://doi.org/10.1016/j.dsr2.2013.01.007

Perhirin, M., Gossner, H., Godfrey, J., Johnson, R., Blanco-Bercial, L., & Ayata, S.-D. (2024). Morphological and taxonomic diversity of mesozooplankton is an important driver of carbon export fluxes in the ocean. *Molecular Ecology Resources*, *24*(2), e13907. https://doi.org/10.1111/1755-0998.13907

Picheral, M., Guidi, L., Stemmann, L., Karl, D. M., Iddaoud, G., & Gorsky, G. (2010). The Underwater Vision Profiler 5: An advanced instrument for high spatial resolution studies of particle size spectra and zooplankton. *Limnology & Oceanography: Methods*, *8*(9), 462–473. https://doi.org/10.4319/lom.2010.8.462

Quiñones, R. A., Platt, T., & Rodríguez, J. (2003). Patterns of biomass-size spectra from oligotrophic waters of the Northwest Atlantic. *Progress in Oceanography*, *57*(3–4), 405–427. https://doi.org/10.1016/s0079-6611(03)00108-3

Richardson, T. L. (2019). Mechanisms and pathways of small-phytoplankton export from the surface ocean. *Annual Review of Marine Science*, *11*(1), 57–74. https://doi.org/10.1146/annurev-marine-121916-063627

Riegman, R., Kuipers, B. R., Noordeloos, A. A., & Witte, H. J. (1993). Size-differential control of phytoplankton and the structure of plankton communities. *Netherlands Journal of Sea Research*, *31*(3), 255–265. https://doi.org/10.1016/0077-7579(93)90026-o

Rodriguez, J., & Mullin, M. M. (1986). Relation between biomass and body weight of plankton in a steady state oceanic ecosystem1. *Limnology & Oceanography*, *31*(2), 361–370. https://doi.org/10.4319/lo.1986.31.2.0361

Rykaczewski, R. R. (2019). Changes in mesozooplankton size structure along a trophic gradient in the California Current Ecosystem and implications for small pelagic fish. *Marine Ecology Progress Series*, *617*, 165–182. https://doi.org/10.3354/meps12554

San Martin, E., Harris, R. P., & Irigoien, X. (2006). Latitudinal variation in plankton size spectra in the Atlantic Ocean. *Deep-Sea Research II*, *53*(14–16), 1560–1572. https://doi.org/10.1016/j.dsr2.2006.05.006

San Martin, E., Irigoien, X., Harris, R. P., Lopez-Urrutia, A., Zubkov, M. V., & Heywood, J. L. (2006). Variation in the transfer of energy in marine plankton along a productivity gradient in the Atlantic Ocean. *Limnology & Oceanography*, *51*(5), 2084–2091. https://doi.org/10.4319/lo.2006.51.5.2084

Scharek, R., Latasa, M., Karl, D. M., & Bidigare, R. R. (1999). Temporal variations in diatom abundance and downward vertical flux in the oligotrophic North Pacific gyre. *Deep-Sea Research Part I-Oceanographic Research Papers*, *46*(6), 1051–1075. https://doi.org/10.1016/s0967-0637(98)00102-2

Selph, K. E., Landry, M. R., Taylor, A. G., Gutiérrez-Rodríguez, A., Stukel, M. R., Wokuluk, J., & Pasulka, A. (2016). Phytoplankton production and taxon-specific growth rates in the Costa Rica Dome. *Journal of Plankton Research*, *38*(2), 199–215. https://doi.org/10.1093/plankt/fbv063

Selph, K. E., Swalethorp, R., R Stukel, M., B Kelly, T., N Knapp, A., Fleming, K., et al. (2021). Phytoplankton community composition and biomass in the oligotrophic Gulf of Mexico. *Journal of Plankton Research*, *44*(5), 618–637. https://doi.org/10.1093/plankt/fbab006

Serra-Pompei, C., Ward, B. A., Pinti, J., Visser, A. W., Kiørboe, T., & Andersen, K. H. (2022). Linking plankton size spectra and community composition to carbon export and its efficiency. *Global Biogeochemical Cycles*, *36*(5), e2021GB007275. https://doi.org/10.1029/2021gb007275

Sheldon, R., Prakash, A., & Sutcliffe, W., Jr. (1972). The size distribution of particles in the ocean 1. *Limnology & Oceanography*, *17*(3), 327–340. https://doi.org/10.4319/lo.1972.17.3.0327

Siegel, D. A., Buesseler, K. O., Behrenfeld, M. J., Benitez-Nelson, C. R., Boss, E., Brzezinski, M. A., et al. (2016). Prediction of the export and fate of global ocean net primary production: The EXPORTS science plan. *Frontiers in Marine Science*, *3*, 22. https://doi.org/10.3389/fmars.2016.00022

Siegel, D. A., Buesseler, K. O., Doney, S. C., Sailley, S. F., Behrenfeld, M. J., & Boyd, P. W. (2014). Global assessment of ocean carbon export by combining satellite observations and food-web models. *Global Biogeochemical Cycles*, *28*(3), 181–196. https://doi.org/10.1002/2013gb004743

Small, L. F., Fowler, S. W., & Unlu, M. Y. (1979). Sinking rates of natural copepod fecal pellets. *Marine Biology*, *51*(3), 233–241. https://doi.org/10.1007/bf00386803

Smayda, T. J. (1971). Normal and accelerated sinking of phytoplankton in sea. *Marine Geology*, *11*(2), 105–122. https://doi.org/10.1016/0025-3227(71)90070-3

Smetacek, V., Klaas, C., Strass, V. H., Assmy, P., Montresor, M., Cisewski, B., et al. (2012). Deep carbon export from a Southern Ocean iron-fertilized diatom bloom. *Nature*, *487*(7407), 313–319. https://doi.org/10.1038/nature11229

Smith, K. L., Jr., Sherman, A. D., Huffard, C. L., McGill, P. R., Henthorn, R., Von Thun, S., et al. (2014). Large salp bloom export from the upper ocean and benthic community response in the abyssal northeast Pacific: Day to week resolution. *Limnology & Oceanography*, *59*(3), 745–757. https://doi.org/10.4319/lo.2014.59.3.0745

Stamieszkin, K., Pershing, A. J., Record, N. R., Pilskaln, C. H., Dam, H. G., & Feinberg, L. R. (2015). Size as the master trait in modeled copepod fecal pellet carbon flux. *Limnology & Oceanography*, *60*(6), 2090–2107. https://doi.org/10.1002/lno.10156

Steinberg, D. K., Carlson, C. A., Bates, N. R., Goldthwait, S. A., Madin, L. P., & Michaels, A. F. (2000). Zooplankton vertical migration and the active transport of dissolved organic and inorganic carbon in the Sargasso Sea. *Deep-Sea Research I*, *47*(1), 137–158. https://doi.org/10.1016/s0967-0637(99)00052-7

Steinberg, D. K., & Landry, M. R. (2017). Zooplankton and the ocean carbon cycle. *Annual Review of Marine Science*, *9*(1), 413–444. https://doi.org/10.1146/annurev-marine-010814-015924

Steinberg, D. K., Van Mooy, B. A. S., Buesseler, K. O., Boyd, P. W., Kobari, T., & Karl, D. M. (2008). Bacterial vs. zooplankton control of sinking particle flux in the ocean's twilight zone. *Limnology & Oceanography*, *53*(4), 1327–1338. https://doi.org/10.4319/lo.2008.53.4.1327

Stemmann, L., & Boss, E. (2011). Plankton and particle size and packaging: From determining optical properties to driving the biological pump.

Stock, C., & Dunne, J. (2010). Controls on the ratio of mesozooplankton production to primary production in marine ecosystems. *Deep-Sea Research I*, *57*(1), 95–112. https://doi.org/10.1016/j.dsr.2009.10.006

Stukel, M. R., Décima, M., Selph, K. E., Taniguchi, D. A. A., & Landry, M. R. (2013). The role of *Synechococcus* in vertical flux in the Costa Rica upwelling dome. *Progress in Oceanography*, *112–113*, 49–59. https://doi.org/10.1016/j.pocean.2013.04.003

Stukel, M. R., & Ducklow, H. W. (2017). Stirring up the biological pump: Vertical mixing and carbon export in the Southern Ocean. *Global Biogeochemical Cycles*, *31*(9), 1420–1434. https://doi.org/10.1002/2017gb005652

Stukel, M. R., Irving, J. P., Kelly, T. B., Ohman, M. D., Fender, C. K., & Yingling, N. (2023). Carbon sequestration by multiple biological pump pathways in a coastal upwelling biome. *Nature Communications*, *14*(1), 2024. https://doi.org/10.1038/s41467-023-37771-8

Stukel, M. R., Kelly, T. B., Aluwihare, L. I., Barbeau, K. A., Goericke, R., Krause, J. W., et al. (2019). The Carbon:^{234}Thorium ratios of sinking particles in the California Current Ecosystem 1: Relationships with plankton ecosystem dynamics. *Marine Chemistry*, *212*, 1–15. https://doi.org/10.1016/j.marchem.2019.01.003

Stukel, M. R., Kelly, T. B., Landry, M. R., Selph, K. E., & Swalethorp, R. (2021). Sinking carbon, nitrogen, and pigment flux within and beneath the euphotic zone in the oligotrophic, open-ocean Gulf of Mexico. *Journal of Plankton Research*, *44*(5), 711–727. https://doi.org/10.1093/plankt/fbab001

Stukel, M. R., Landry, M. R., Benitez-Nelson, C. R., & Goericke, R. (2011). Trophic cycling and carbon export relationships in the California Current Ecosystem. *Limnology & Oceanography*, *56*(5), 1866–1878. https://doi.org/10.4319/lo.2011.56.5.1866

Taylor, A. G., Goericke, R., Landry, M. R., Selph, K. E., Wick, D. A., & Roadman, M. J. (2012). Sharp gradients in phytoplankton community structure across a frontal zone in the California Current Ecosystem. *Journal of Plankton Research*, *34*(9), 778–789. https://doi.org/10.1093/plankt/fbs036

Taylor, A. G., & Landry, M. R. (2018). Phytoplankton biomass and size structure across trophic gradients in the southern California Current and adjacent ocean ecosystems. *Marine Ecology Progress Series*, *592*, 1–17. https://doi.org/10.3354/meps12526

Taylor, A. G., Landry, M. R., Freibott, A., Selph, K. E., & Gutierrez-Rodriguez, A. (2016). Patterns of microbial community biomass, composition and HPLC diagnostic pigments in the Costa Rica upwelling dome. *Journal of Plankton Research*, *38*(2), 183–198. https://doi.org/10.1093/plankt/fbv086

Thornton, D. C. O. (2002). Diatom aggregation in the sea: Mechanisms and ecological implications. *European Journal of Phycology*, *37*(2), 149–161. https://doi.org/10.1017/s0967026202003657

Turner, J. T. (2015). Zooplankton fecal pellets, marine snow, phytodetritus and the ocean's biological pump. *Progress in Oceanography*, *130*, 205–248. https://doi.org/10.1016/j.pocean.2014.08.005

Volk, T., & Hoffert, M. I. (1985). Ocean carbon pumps: Analysis of relative strengths and efficiencies in ocean-driven atmospheric CO_2 changes. In E. T. Sundquist & W. S. Broeker (Eds.), *The carbon cycle and atmospheric CO_2: Natural variations Archean to present* (pp. 99–110). American Geophysical Union.

Waite, A. M., Safi, K. A., Hall, J. A., & Nodder, S. D. (2000). Mass sedimentation of picoplankton embedded in organic aggregates. *Limnology & Oceanography*, *45*(1), 87–97. https://doi.org/10.4319/lo.2000.45.1.0087

Ward, B. A., Dutkiewicz, S., Jahn, O., & Follows, M. J. (2012). A size-structured food-web model for the global ocean. *Limnology & Oceanography*, *57*(6), 1877–1891. https://doi.org/10.4319/lo.2012.57.6.1877

Yingling, N., Kelly, T. B., Shropshire, T. A., Landry, M. R., Selph, K. E., Knapp, A. N., et al. (2022). Taxon-specific phytoplankton growth, nutrient limitation, and light limitation in the oligotrophic Gulf of Mexico. *Journal of Plankton Research*, *44*(5), 656–676. https://doi.org/10.1093/plankt/fbab028